



FLEXURAL BEHAVIOR OF SEAWATER FERROCEMENT CONCRETE BEAMS REINFORCED BY GFRP BARS AND FIBERGLASS MESH

Mohamed Hatem^{1,2}, Nader Mohamed¹, Khaled Samy², Mohamed Abdelrazik¹

¹ Department of Civil Engineering, Faculty of Engineering, Al-Azhar University, Cairo, Egypt,

² Department of Civil Engineering, Faculty of Engineering, Higher Institute for Engineering, 5th settlement, Cairo, Egypt,

*Correspondence: mohamedelserwy@azhar.edu.eg

Citation:

M. Hatem, N. Mohamed, K. Samy and M. Abdelrazik" Flexural Behavior of SEAWATER Ferrocement Concrete Beams Reinforced by GFRP bars and Fiberglass Mesh", Journal of Al-Azhar University Engineering Sector, vol. 20, No. 74, 2025, 1-16.

Received: 18 May 2024

Revised: 31 August 2024

Accepted: 02 October 2024

Doi:10.21608/aej.2024.290793.1666

Copyright © 2025 by the authors. This article is an open-access article distributed under the terms and conditions of Creative Commons Attribution-Share Alike 4.0 International Public License (CC BY-SA 4.0)

ABSTRACT

This study investigates the potential of seawater as a sustainable and economical alternative to freshwater in producing ferrocement beams. These beams aim to surpass conventional reinforced concrete beams in terms of load resistance, crack prevention, and environmental impact. The experiment work involved four groups of ferrocement beams, all reinforced with fiberglass mesh. The investigation focused on the effects of varying the water-to-cement ratio and seawater content within the concrete mix design. Six concrete specimens (1600 mm x 300 mm x 150 mm) were cast, incorporating fiberglass bars and mesh for reinforcement. The first group contains control beam cast with potable water, the second group contains beam cast with a specific percentage of seawater content in the concrete mix, the third group contains two beams cast with a specific percentage of seawater content and reduced reinforcement ratio and the forth group contains two beams cast with a specific percentage of seawater content, reduced reinforcement ratio, and increased mesh layers. The cracking load, load-deflection behavior, energy absorption capacity, and cracking patterns have been evaluated for the four groups. The results revealed that increasing the seawater content led to a 7% increase in concrete strength and a 3% to 20% increase in ultimate load capacity increase in energy absorption ranging from 31% to 83%.

KEYWORDS: Ferrocement Concrete, Green Concrete, Fiber Glass, Sea Water.

سلوك انحناء الكمرات الفيروسمنتيه باستخدام مياه البحر و المقواه بقضبان الألياف والشبكة الزجاجية

محمد حاتم^{1,2*}، نادر محمد¹، خالد سامي²، محمد عبد الرازق¹

¹ قسم الهندسة المدنية، كلية الهندسة، جامعة الأزهر، مدينة نصر، 11884، القاهرة، مصر.

² قسم الهندسة المدنية، المعهد العالي للهندسة و التكنولوجيا، التجمع الخامس، القاهرة، مصر.

*البريد الإلكتروني للباحث الرئيسي : mohamedelserwy@azhar.edu.eg

الملخص

تدرس هذه الدراسة إمكانية استخدام مياه البحر كبديل مستدام واقتصادي للمياه العذبة في إنتاج كمرات الفيروسمنتيه. تهدف هذه العوارض إلى التفوق على عوارض الخرسانة المسلحة التقليدية من حيث مقاومة الحمل ومنع التشقق والأثر البيئي. اشتملت التجربة

على أربع مجموعات من الكمرات الفيروسمنتية، وكلها معززة بشبك من الألياف الزجاجية. ركز البحث على تأثيرات تغيير نسبة الماء إلى الأسمنت ومحتوى مياه البحر داخل تصميم خليط الخرسانة. تم صب ست عينات خرسانة (1600 مم × 300 مم × 150 مم)، تتضمن قضبان وشبكة من الألياف الزجاجية للتعزيز. المجموعة الأولى تتضمن كمره مصبوبة بالمياه الصالحة للشرب، المجموعة الثانية تتضمن كمره مصبوبة بنسبة معينة من محتوى مياه البحر في خليط الخرسانة، المجموعة الثالثة تتضمن كمرتين مصبوبتان بنسبة معينة من محتوى مياه البحر ونسبة تسليح مخفضة، المجموعة الرابعة تتضمن كمرتين مصبوبتان بنسبة معينة من محتوى مياه البحر ونسبة تسليح مخفضة وطبقات شبكة زائدة. تم تقييم حمل التشقق وسلوك الحمل والانحراف وقدرة امتصاص الطاقة وأنماط التشقق للمجموعات الأربعة. وأظهرت النتائج أن زيادة محتوى مياه البحر أدت إلى زيادة بنسبة 7% في قوة الخرسانة وزيادة تتراوح من 3% إلى 20% في سعة الحمل النهائية وزياده ملحوظه في امتصاص الطاقه تتراوح من 31% الي 83%

الكلمات المفتاحية: خرسانة الفيروسمنت ، الخرسانة الخضراء ، الألياف الزجاجية ، مياه البحر .

1. INTRODUCTION

Concrete is considered the most used building material around the world and it consumes more than a billion tons of fresh water and with the spread of concrete use, more and more fresh water will be consumed. Studies have shown that more than half of the world's population may lack fresh water by 2025 [1]. The construction industry consumes a significant amount of freshwater, estimated at over 2 billion tons annually. In areas grappling with water shortages, often exacerbated by natural disasters, this freshwater use can be a major concern. Seawater, on the other hand, presents a viable alternative for mixing concrete. In the last few years, The construction industry's reliance on freshwater is a growing concern. Globally, concrete production devours a staggering 9% of industrial water use. Forecasts predict a worrying trend – by 2050, 75% of the water needed for concrete will be required in regions already grappling with water scarcity. Freshwater limitations and the environmental drawbacks of desalination are pushing the industry towards innovative solutions. Seawater, once considered unsuitable, is emerging as a viable alternative for mixing concrete. This shift has the potential to significantly reduce freshwater consumption in construction, paving the way for a more sustainable future.

Seawater accounts for about 96.5% of the world's accessible water, it presents a compelling alternative to freshwater for concrete production, particularly in coastal regions where freshwater resources are scarce. As a renewable resource, unlike freshwater which is generally considered nonrenewable, seawater offers a more sustainable long-term solution for concrete mixing [2].

The concrete structures are weakened when exposed to chemicals, causing them to deteriorate rapidly. This reduces their lifespan and necessitates costly repairs and maintenance. Chemical attack is also a major culprit behind steel corrosion in reinforced concrete. There are many solutions to this problem, one approach involves using concrete designed for seawater environments that doesn't incorporate steel reinforcement. Another option is to employ corrosion-resistant materials, such as fiber-reinforced polymers (FRP), in place of traditional steel reinforcement [3].

The possibility of using seawater for mixing concrete holds significant appeal. Studies suggest past success with seawater concrete, particularly in coastal regions like Southern California and Florida [4]. This approach could offer environmental and economic benefits by reducing reliance on fresh water. This study investigated the effect of seawater on concrete strength, using Ordinary Portland Cement (OPC) [5]. While seawater can be an attractive alternative for mixing or curing concrete which alters the rate of strength gain. The concrete specimens prepared and cured with fresh water exhibited a strength reduction of approximately 15% at 90 days less than those prepared using seawater

The possibilities of using seawater in concrete has been investigated which indicated that it is a key consideration lies in its potential application. Studies suggest that seawater might be more suitable for unreinforced concrete and mortar, which constitute a significant portion (around 55%) of cement-based construction materials [6]. Examples include bricklaying mortar, renders, and other non-structural elements. Studies investigating the viability of seawater concrete often raise concerns about its long-term performance. However, real-world examples offer encouraging evidence. Several unreinforced concrete structures along the coasts of Florida and Los Angeles, prepared using seawater for mixing and curing processes, have revealed no significant signs of degradation [7, 8].

Seawater offers an attractive alternative for mixing concrete that shown a trade-off in strength compared to fresh water. However, this potential drawback might be addressed through the use of Glass Fiber Reinforced Polymer (GFRP). Reinforcement GFRP exhibits significant promise as a replacement for traditional steel rebar in chloride-rich environments like marine structures [9].

To unlock the broader application of concrete mixed with seawater, a comprehensive understanding of its behavior when combined with embedded GFRP bars is crucial. While extensive research exists on the durability of GFRP bars themselves [10-16].

On the other hand, the ferro-cement beams while has gained renewed interest as a construction material. The American Concrete Institute (ACI) Committee 549 has a long-standing definition established in 1971 [17]. According to ACI, ferrocement is a type of reinforced concrete typically constructed using a mortar matrix of hydraulic cement. This mortar is reinforced with closely spaced layers of fine wire mesh. The mesh can be metallic or composed of other suitable materials. Importantly, the fineness and composition of the mortar matrix should be compatible with the size and spacing of the reinforcing mesh to ensure proper encapsulation. The mortar matrix may also incorporate discontinuous fibers for additional reinforcement [18, 19].

Erfan, A.M., Abd Elnaby, R.M., Elhawary, A. and El-Sayed, T.A., 2021 [25] Investigated The incorporation of ferrocement composites into reinforced concrete (RC) walls significantly enhances their compressive behavior under both centric and eccentric loading conditions. Experimental and numerical results consistently demonstrated that ferrocement reinforcement, particularly with glass fiber wire mesh, leads to improved load-carrying capacity, ductility, and energy absorption compared to control specimens. The finite element analysis accurately predicted the structural performance of these composite walls, validating the experimental findings.

In a study by El-Sayed, T.A. and Erfan, A.M., 2018 [26] The study demonstrated the effectiveness of ferrocement as shear reinforcement in concrete beams. Replacing a portion of traditional stirrups with wire mesh was found to increase shear capacity compared to beams with only stirrups or expanded metal mesh. The experimental and numerical results showed a strong correlation, validating the analytical approach. While welded wire mesh exhibited the highest shear strength, further research is needed to optimize the type and distribution of ferrocement reinforcement for maximum efficiency. This study provides valuable insights into the potential of ferrocement as a viable alternative or complement to traditional shear reinforcement in concrete structures.

The effect of number of mesh layers and steel mesh type on the performance of U-shaped ferrocement formwork beams has been studied [20]. The results revealed that these beams exhibited superior performance, characterized by increased ultimate and serviceability load capacity, improved crack control, enhanced ductility, and greater energy absorption. These findings

align with similar observations reported by Shaheen and Eltehawy [21]. The flexural behavior of solid and hollow reinforced concrete beams has been investigated [22]. Six beams, each measuring 200mm x 300mm x 2300mm, were tested. Two beams were solid, while the remaining four had a longitudinal circular hollow section positioned below the calculated neutral axis. Concrete of M30 grade was used for all specimens. The beams were subjected to gradually increasing two-point loading, and a Linear Variable Displacement Transducer (LVDT) was employed to measure the resulting deflection. It can be concluded that the flexural behavior of the hollow-core beams closely resembled that of conventional reinforced concrete beams.

The stress-strain behavior of lightweight fiber-reinforced ferrocement specimens under uniaxial tension has been investigated [23]. It is revealed that the inclusion of fibers in the ferrocement specimens resulted in failure by a single dominant crack. This suggests that fiber-reinforced ferrocement members in tension behave more like a homogenous material, in contrast to specimens made solely of ferrocement.

The effect of jute fibers on the impact behavior of ferrocement slabs (500 x 500 x 50 mm) through experimental testing has been investigated. These slabs were compared to those of unreinforced control slabs. The test results reveal a significant improvement in impact resistance with jute fiber reinforcement. The configuration using 50 mm wide strips in a crisscross pattern yielded the best performance. Compared to the control slabs, this configuration increased the first crack load by 722.58%, the slight separation load by 232.26%, and the full perforation load by 206.18% [24].

Studies in (2020) [27] by Erfan, T.A. These findings suggest that GFRP reinforcement is a viable and effective alternative to traditional steel reinforcement for deep beam applications, offering advantages such as improved durability and corrosion resistance.

The current study aims at studying the Structural Behavior of the ferrocement beams using sea water and replace it instead of the conventional concrete beams using sea water that have a high ability to resist loads and cracks. The effect of using fresh water and replace it with sea water was also investigated in order to save the fresh water.

2. Materials and Methods

2.1. Materials

The materials used in the current study include Sulfate Resistance Cement, Al Tameer Cement (CEMI-42.5 N) Giza, Egypt. The natural siliceous sand was chosen as a fine aggregate. Two types of water were used in preparing the mixes, the first type was clean drinking fresh water was obtained from the tap that is free from impurities, the second type was sea water obtained from red sea, Ain-Sokhna, Egypt. For each cement content reasonable water / cement ratio was decided upon after carrying out many different control tests to ensure that the different resulting mixes will have the same adequate plasticity. Silica fume of commercial grade was obtained from Sika Company, Cairo, Egypt. The fiber mesh purchased from Geosegypt Company's fiber mesh e300, Cairo, Egypt.

2.2. Materials charactisation

The main compounds, chemical constituents, physical characteristics, specific weight, bulk density, soundness and alkali equivalent of the used sulfate resistance cement (cemi-42.5 n) has been determined as presented in **Table 1**.

Table 1. Physical properties of Sulphate Resist Cement.

Test Description	Test Result	Specification Limits
Percentage of water to give a paste of standard consistency, w/c %	45 %	
Setting time (Vicat test) - Initial - Final	Hr : min 1 : 30 4 : 45	Not less than 45 min Not more than 10 hr
Soundness of cement (Le Chatelier test)	5 mm	Not more than 10 mm
Fineness of cement, Percentage retained on the Standard 0.09 mm sieve by weight	8 %	Not more than 10 %
Compressive strength of Mortar 7x7 cm cubes - 2 days - 28 days	200 kg/cm ² 520 kg/cm ²	Not less than 150 kg/cm ² Not less than 470 kg/cm ²

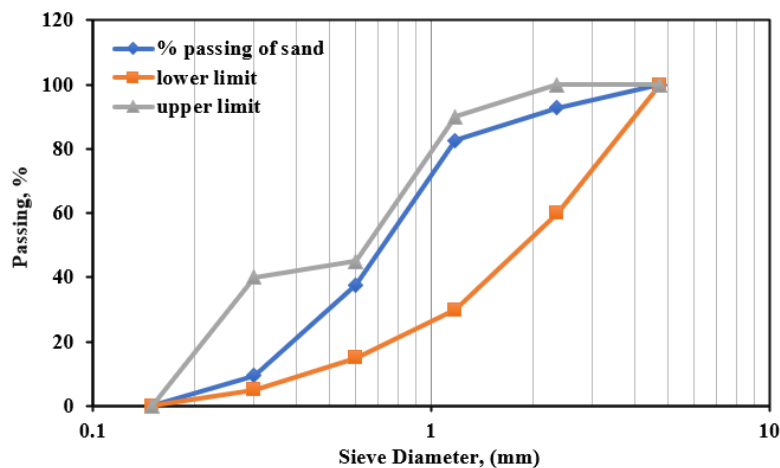
The natural siliceous sand was used as fine aggregate is clean and nearly impurity-free, with 2.6 specific gravity and 2.91 modulus of fineness. It is clear that the sand's characteristics are in agree with the E.S.S. 1109/2008. The characteristics of the sand used are shown in **Table 2**, and the grading of the sand is shown in **Table 3** and **Fig. 1**.

Table 2. Properties of the used fine aggregate.

Property	Test results for Sand
Specific Gravity	2.6
Unit Weight	1.7
Fineness Modulus	2.91
Clay, Silt, and Fine Dust	2% (by weight)
Chloride Percent	0.03 (by weight)

Table 3. Sieve analysis of the used fine aggregates.

Sieve Diameter (mm)	4.75	2.36	1.18	0.6	0.3	0.15
% Passing	100	92.8	82.6	37.7	9.50	0
% Passing (E.S.S. 1109/2008) (Medium Zone)	100	60-100	30-90	15-45	5-40	0

**Fig. 1. Grading curve of the used sand.**

The two types of mixing water was analysed chemically using Inductively coupled plasma mass spectrometry (ICP-MS) to determine chlorides, sulfates, alkalinity, total dissolved solids, and pH (at 25°C). These Measurements were compared according to the Egyptian specifications as shown in **Table 4**.

Table 4. Chemical properties of the used mixing water.

Test	Unit	Maximum limit (ECP)	Results	
			Fresh water	Seawater
Chloride (Cl ⁻)	Ppm	500	52	25000
Sulfate (SO ₄ ⁻²)	ppm	300	56.28	4357
Total dissolved solids (TDS)	ppm	2000	342.54	51285
pH (at 25 °C)	-	Not less than 7	7.62	7.38
Turbidity	-	-	.51	1.38
HCO ₃	ppm	1000	140	130

The used silica fume is typically powder of gray-color that resembles Portland cement or fly ashes. It has a powder form and had a light grey color. **Table 5** lists the physical characteristics and chemical composition of the used silica fume according to Sika Company. Condensed silica fume is utilized as a partial replacement for cement in mortar to increase the permeability and the strength and of the mortar matrix.

Table 5. Physical properties and chemical composition of used Silica Fume.

Form	Powder solid
Color	grey
Boiling point/boiling range	Not applicable
Flammability (solid, gaseous)	The product is not flammable
Bulk density	300 kg/m ³
Density	250-350 kg/m ³
Specific gravity	2.2

The fiber mesh used in the current study is shown in **Table 6** which shows the chemical and physical characteristics of the Geosegypt Company's fiber mesh e300. Fibers are frequently used to avoid cracking, which is a result of drying shrinkage and heat expansion/contraction. Additionally, it was utilized to provide fibrillated toughness and residual strength to concrete, increase impact resistance, shatter resistance, and abrasion resistance.

Table 6. Chemical and physical properties of polypropylene fiber e300.

Absorption	Nil
Type/ shape	Graded/ Fibrillated
Specific Gravity	0.91
Fiber Length	Various
Electrical Conductivity	Low
Acid & Salt Resistance	High
Melting Point	324°F (162°C)
Thermal Conductivity	Low
Ignition Point	1100°F (593°C)
Alkali Resistance	Alkali Proof

A high-range water-reducing (HRWR) admixture (Sikament 163 M) was used to produce concrete with a high workability. The technical characteristics of the admixture utilized, according to the manufacturer, are listed in **Table 7**.

Table 7. Technical properties of the admixture used (at 25°C).

Base	Naphthalin sulphonate
Appearance	Brown liquid
Density	Approx. 1.2 kg/lit
Chloride content	Nil
Air entrainment	Nil
Compatibility	All types of Portland cement

The GFRP bars used in this study were produced by ARMASTEK® _Russia and were contrived by the pultrusion method of E-glass fibers immersed in modified vinyl ester resin. A 10-mm rebar glass fiber reinforced polymer (GFRB) manufactured by Russian Company Armastek was used ,are listed in **Table 8**
, Stress-Strain Curve of GFRP rebar and Mesh as shown in in **Fig 2,3** .

Table 8. Technical properties of GFRP.

Parameter	FGM	GFRP-Rebar
Density, kg/m3	1210	1900
Modulus of elasticity (Es), MPa	80000	50000
Poisson's ratio (ν)	0.3	0.25
Ultimate strength, MPa	325	1000

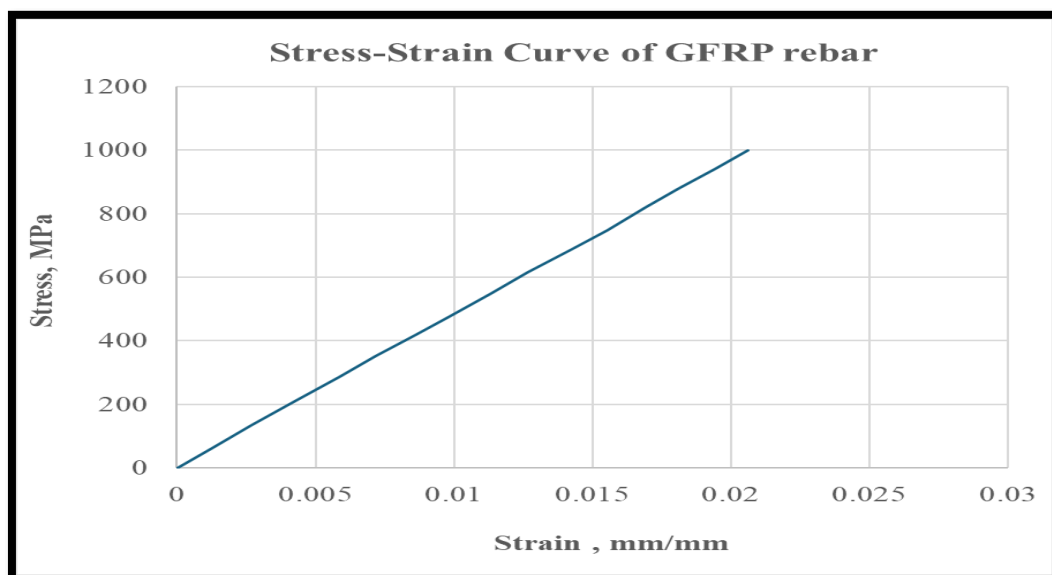


Fig. 2. Stress-Strain Curve of GFRP rebar.

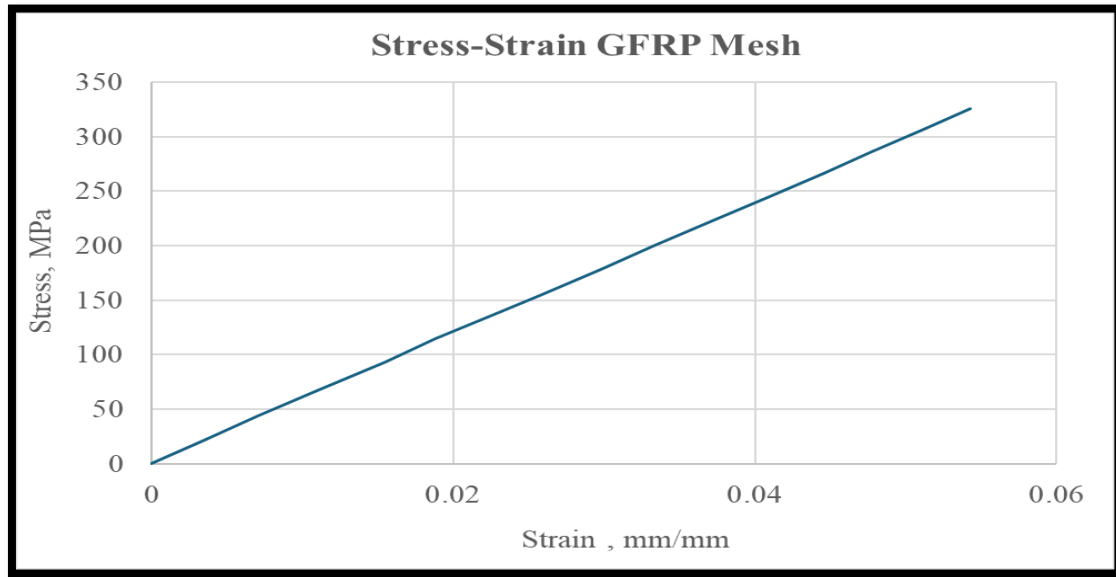


Fig. 3. Stress-Strain Curve of GFRP Mesh.

2.3. Method

2.3.1. Mix design

Six specimens, one control ferrocement beam with fresh water in concrete mix and three ferrocement beam with sea water in concrete mix were prepared and cast in the laboratory of Resistance and Testing of Materials at Housing and Building National Reserch Center (HBRC), Cairo, Egypt. All specimens have the same dimensions of 150×300×1600 mm with virous types of Mixing water ratio as shown in Fig. 4. The specimens were loaded in flexure under a two-point loading system with a simply supporting conditions up to failure as explained in Table 9.

The concrete mortar used for ferro-cement beams was designed to achive the ultimate compressive strength after 28-days curing time of 35 MPa (350 kg/cm²). The properties of the mix for mortar matrix were chosen according to the (ACI committee 549 report: 1988) [1]. stress-strain relationship for the ferrocement shown in Fig5 .The matrix of ferro cement is mortar that consists of cement, water, sand and optionally an admixture portland cement, fine grained sand, sea water and GFRP meshes. In mortar production, cement type will depend on source of sea water and the properties of sand, cement. Admixture was used as mortar super plasticizer to ensure the workability as shown in Table 10. Despite the small aperture of square wire mesh, the mortar was easily placed in molds.

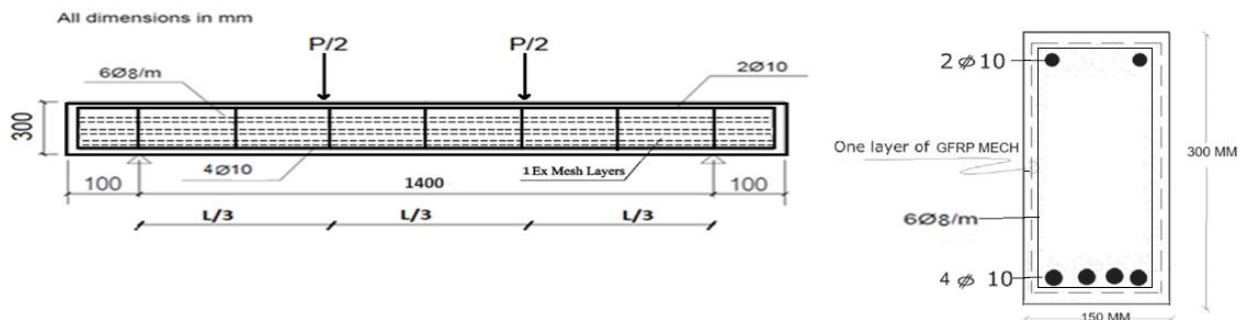


Fig. 4. Reinforcement and dimensions of tested specimens.

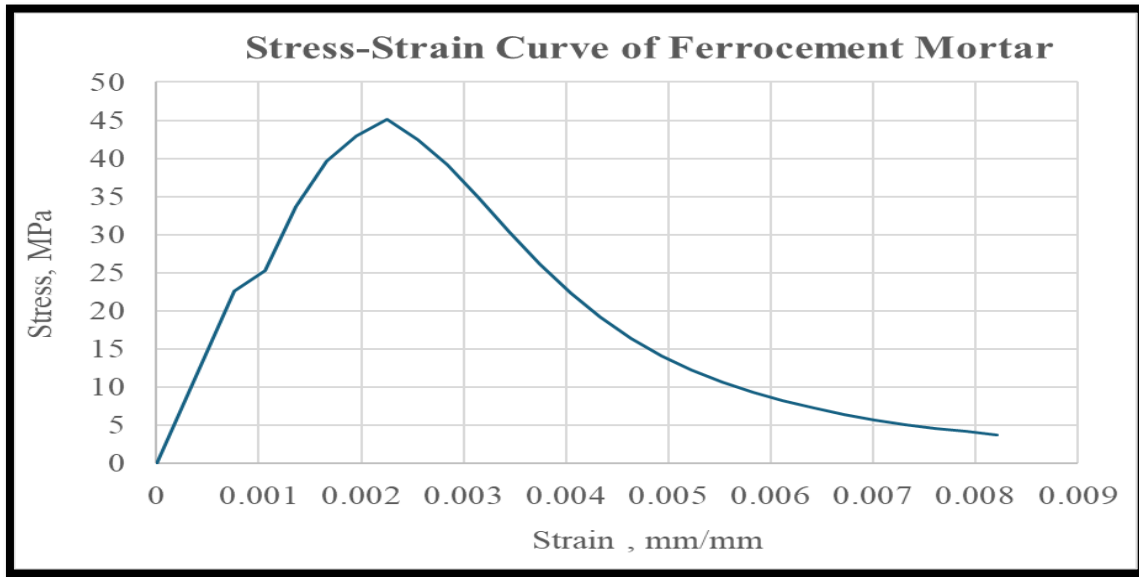


Fig. 5. Stress-Strain Curve of Ferrocement Mortar.

Table 9. Details of different groups of the mix.

Group	Beam	% Sea Water Mixing	% Sea Water Treatment	Reinforcement	Mech Layer	Parameter
1	B1	0	0	2Φ10 Upper 4Φ10 Lower	1 Layer	- Control
2	B2	100	0	2Φ10 Upper 4Φ10 Lower	1 Layer	-Percentage of Sea Water Mixing
3	B3	100	0	2Φ10 Upper 3Φ10 Lower	1 Layer	- Percentage of Reinforcement
	B4	100	0	2Φ10 Upper 2Φ10 Lower	1 Layer	- Percentage of Sea Water Mixing
4	B5	100	0	2Φ10 Upper 2Φ10 Lower	2 Layer	-Percentage of Reinforcement
	B6	100	0	2Φ10 Upper 2Φ10 Lower	3 Layer	-Percentage of Sea Water Mixing -Mech Layer

Table 10. Mortar mix quantities.

MIX Design	Cement (kg/m ³)	Sand (kg/m ³)	Water (kg/m ³)	Super plasticizer (kg/m ³)	Silica fume (kg/m ³)	Fibers (kg/m ³)
Ratio from cement weight	1	2.2	0.4	0.01	0.1	0.0024
M1	626.4	1392	243.6	10.44	69.6	1.5

2.3.3. Preparation and Casting

For casting samples, wooden molds were used with the appropriate dimensions as shown in Fig. 6. The reinforcing fiber glass and fiber glass mesh were prepared outside the wooden mold with the required dimensions and details. It is worth mentioning that the concrete was cast after mixing for a period of between 10 and 12 minutes.



Fig. 6. Preparation and casting processes.

2.3.4. Test Setup

The RC beam specimens testing in flexure was conducted after 365 days. All the tested beams were totally coated with white plastic paint to detect cracks during the testing procedure. The universal testing machine of 5000 kN load capacity was applied using the uniform ramping increments up to failure and the loading rate was 15KN/min as presented in **Fig. 7**. A linear variable displacement transducer (LVDT) placed under the center point of the tested beam specimens was used to continuously recorded the mid-span deflection as presented in **Fig. 8**. The readings of deflection and strains were automatically recorded at each load stage, using a Data Logger connected to a computer as shown in **Fig. 8**. At each load stage, the crack pattern was also tracked and marked. During the load application, the general structural behavior of the tested beam specimens was carefully observed. When excessive cracking take place at the bottom of the beam, the failure load is identified, the applied load drops and hence the deflection increases. A trial mixes will be test according to the previous researches as shown in **Table 11**.

Table 11. The Compression test data of the tested beams.

Period (days)		Slump	7 days	365 days
		(mm)	Peak compressive strength (MPa)	
Cubic for specimen no.	B1	23	29.1	43.17
	B2	22	30.5	46.20
	B3	22	30.5	46.20
	B4	22	30.5	46.20
	B5	22	30.5	46.20
	B6	22	30.5	46.20

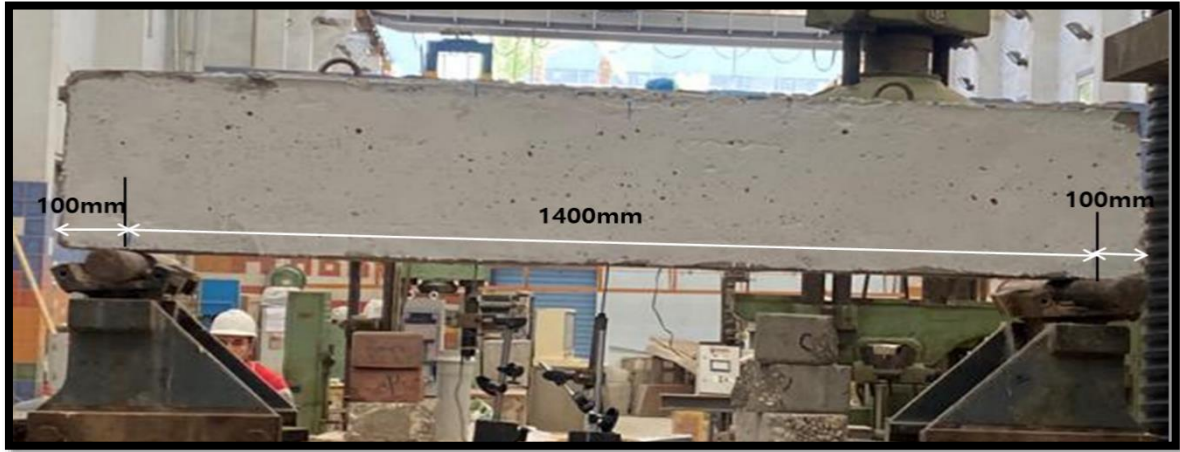


Fig. 7. Test setup configurations.

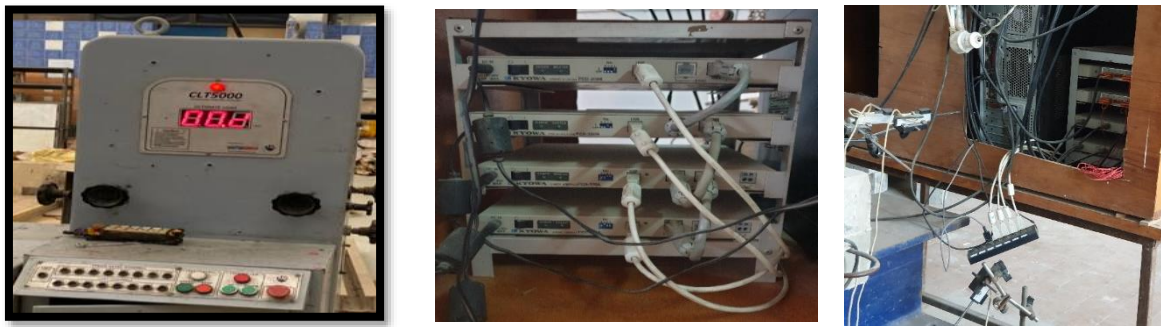


Fig. 8. Data logger system.

3. RESULTS AND DISCUSSION

3.1. Mechanical Properties

Table 12 condenses the key findings from the experiment, including the ultimate breaking point (ultimate failure load) and the initial crack point (first crack load) for each concrete beam specimen. Additionally, it presents a measure of the beam's flexibility (ductility ratio) and its total capacity to absorb energy (energy absorption). Fig. 9 visually depicts the relationship between the applied load and the resulting deflection of the beams.

Table 12. Comparison of flexural behavior results.

Group	Beam	First Crack Load (P _{cr})		Ultimate Load (P _u)		Deflection at First Crack (δ _{cr})		Deflection at Ultimate (δ _u)		Energy Absorption Capacity	
		Measured (kN)	Relative (%)	Measured (kN)	Relative (%)	Measured (mm)	Relative (%)	Measured (mm)	Relative (%)	Measured (kN.mm)	Relative (%)
1	B1	36.10	100%	187.11	100%	0.99	100%	16.11	100%	1,920.79	100%
2	B2	45.07	125%	223.82	120%	1.76	178%	24.15	150%	3,508.36	183%
3	B3	35.90	99%	180.07	96%	0.37	38%	22.19	138%	2,739.42	143%
	B4	33.47	93%	138.80	74%	1.11	112%	25.67	159%	2,520.41	131%
4	B5	35.30	98%	173.60	93%	1.23	125%	27.11	168%	3,141.42	164%
	B6	40.23	111%	191.70	102%	1.25	127%	27.68	172%	3,541.13	184%

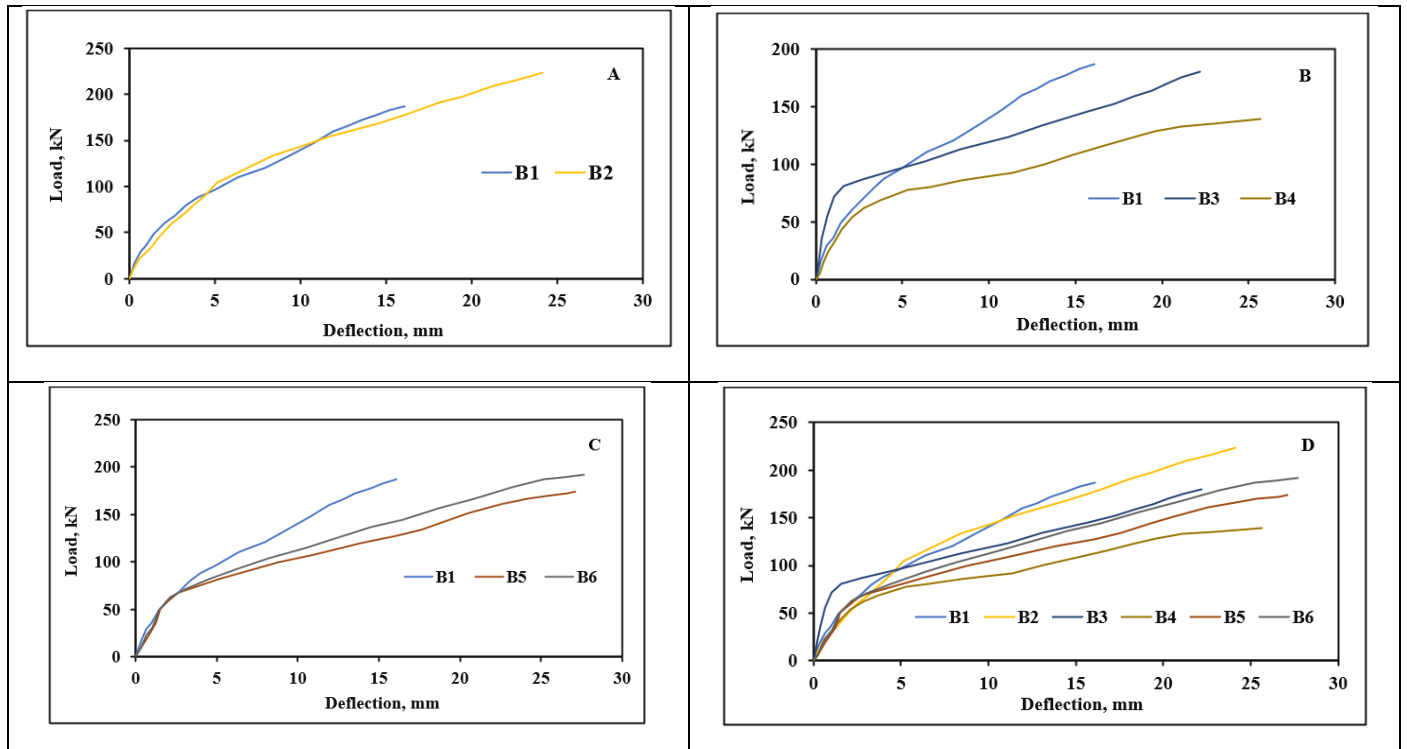


Fig. 9. Load-Deflection curve of tested specimens where A) for group one and group two, B) for group one and group three ,C) for group one and group four, D) for all groups.

as shown in **Fig. 10** Group Two (Seawater Mix): Compared to the control group, all beams containing seawater in the concrete mix (Group Two) exhibited a significant increase in ultimate load, roughly around 20%. This suggests a potential benefit of using seawater in the concrete mix for enhancing load-bearing capacity.

Group Three (Reduced Reinforcement): Conversely, beams in Group Three with reduced reinforcement displayed a decrease in ultimate load. This reduction varied, ranging from approximately 4% to a more substantial 26%. This finding highlights the importance of adequate reinforcement for optimal load-bearing capacity.

Group Four (Combined Effects): Group Four explored the combined effects of reduced reinforcement and additional mesh layers. Beam 5 in this group experienced a decrease in ultimate load of around 7%, likely due to the combined influence of both factors. However, Beam 6 displayed a surprising 3% increase in ultimate load despite the reduced reinforcement. This suggests that the presence of three mesh layers might have played a role in counteracting the negative impact of reduced reinforcement.

Energy absorption, a measure of a beam's ability to absorb energy before breaking, is calculated as the shaded area under the load-deflection curve. The area under the curve was calculated using a computer program (BASIC language) by integrating the equation of the load-deflection curve for each beam specimen as follows:

$$\text{Ultimate load Energy absorbed} = \int_0^{\Delta_u} f(\Delta) d\Delta$$

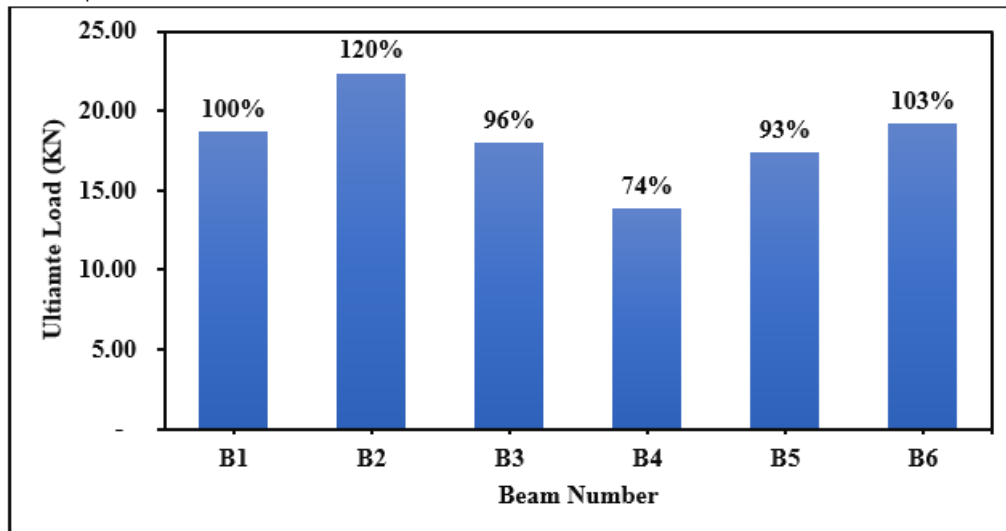


Fig. 10. Ultimate loads values of all tested beams.

Where $f(\Delta)$ is the equation of the load-deflection curve, and Δ_u is the mid-span deflection at failure load, as shown in **Fig. 11**. A larger shaded area indicates a higher capacity for energy absorption.

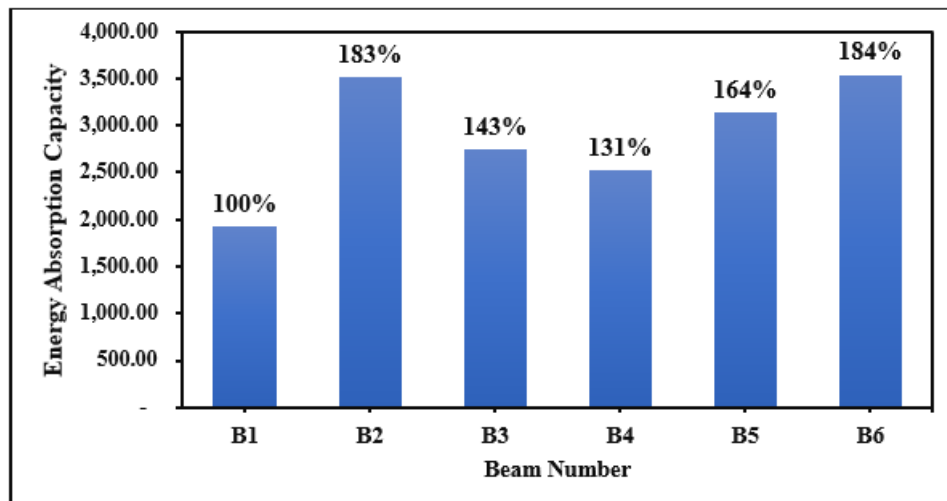


Fig. 11. Energy absorption capacity of all tested beams.

While detailed data is available in **Table 12**, analyzing the figures reveals that beam B6 in Group Four outperformed all other beams in terms of energy absorption. This suggests a potential benefit for beams in Group Four, prompting further investigation into the specific design features that contribute to this improved energy absorption.

The experiment also compared the energy absorption of different beam groups to a control group. Here's a breakdown of the findings:

Group Two: Increased energy absorption by 83% compared to the control group.

Group Three: Showed the most significant improvement, with increases of 31% and 43% compared to the control group.

Group Four: Increased energy absorption by 64% to a maximum value of 84%, surpassing all other groups.

This reformulated version simplifies the explanation of energy absorption and highlights the key findings:

B6 in Group Four has the highest energy absorption. Group Three shows the most significant improvement compared to the control group. Group Four offers a promising design approach due to its high energy absorption.

Fig. 12 show cases the cracking patterns observed in the tested beams.

Control Group: Cracks began near the center of the beam (mid-span) and grew rapidly towards the opposite side (compression side) as the load increased. These cracks eventually ran the entire length of the beam. Groups Two and Three: Similar to the control group, the first crack appeared near the center for these groups as well. The exact load at which this crack occurred (first crack load) varied depending on the amount of seawater used in the concrete mix as detailed in **Table 12**. Group Four: The first crack also initiated near the center in this group. However, the first crack load was influenced by two factors: the amount of seawater and the combined effect of less reinforcement on the bottom and the addition of mesh layers.

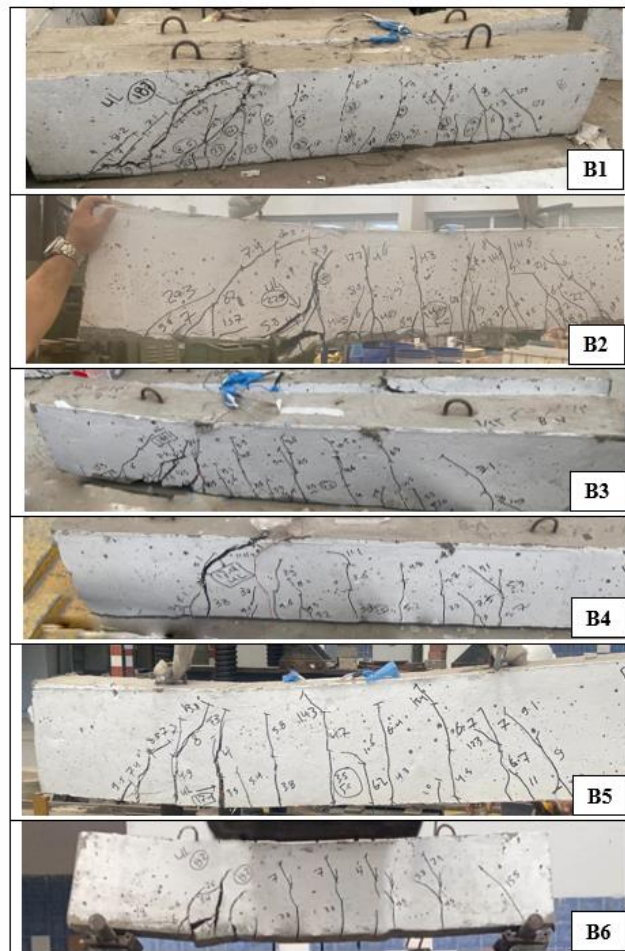


Fig. 12. Ultimate loads values of all tested beams.

Conclusion

- Compared to the control group, beams containing seawater throughout the concrete mix exhibited a significant increase in ultimate load.
- Seawater enhanced Ferrocement concrete's performance, including its energy absorption capacity, compared to the control.

- testing after 365 days had a positive effect on ferrocement concrete in the ultimate load and energy absorption of the specimens .
- While seawater improved performance, it's important to note that beams with higher seawater content also displayed a greater number of cracks
- As expected, decreasing the reinforcement ratio lead to reduction in the maximum load of the beams could withstand (ultimate load).
- increasing the number of mesh layers in Ferrocement Beams using sea water in mixing can mitigate the negative impact of reduced reinforcement on the ultimate load.

References

1. WHO, W.H.O., Global water supply and sanitation assessment 2000 report. 2000, World Health Organization (WHO) and the United Nations Children's Fund (UNICEF): Geneva.ACI Committee 549. (1997). State-of-the-Art Report on Ferrocement. ACI 549R-97, 1–26.
2. Gleick, P. H. (1993). Water in crisis (Vol. 100). New York: Oxford University Press.
3. Younis, A., Ebead, U., & Nanni, A. (2017). A perspective on seawater/frp reinforcement in concrete structures. ISEC 2017
4. Nobuaki Otsuki, Tsuyoshi Saito, & Yutaka Tadokoro. (2012). Possibility of Sea Water as Mixing Water in Concrete. Journal of Civil Engineering and Architecture, 6(11).
5. Guo, Q., Chen, L., Zhao, H., Admilson, J., & Zhang, W. (2018). The effect of mixing and curing seawater on concrete strength at different ages. In MATEC Web of Conferences (Vol. 142, p. 02004). EDP Sciences.
6. Scrivener, K.L., V.M. John, and E.M. Gartner, Eco-efficient cements: Potentially economically viable solutions for a low-CO₂ cement-based materials industry. Cement and Concrete Research, 2018.
7. Hadley, H., Letter to editor, in Engineering News-Record. 1935. p. 716-717.
8. ACI, Job problems and practice. 1940, American Concrete Institute. p. 313-314.
9. Nanni, A., A. De Luca, and H.J. Zadeh, FRP reinforced concrete structures—theory, design and practice. 2014, Boca Raton, FL: CRC Press.
10. Zhou, J., X. Chen, and S. Chen, Effect of different environments on bond strength of glass fiber-reinforced polymer and steel reinforcing bars. KSCE Journal of Civil Engineering, 2012. 16(6): p. 994-1002.
11. Chen, Y., et al., Accelerated aging tests for evaluations of durability performance of FRP reinforcing bars for concrete structures. Composite Structures, 2007. 78(1): p. 101-111.
12. Hao, Q., et al., Bond strength of glass fiber reinforced polymer ribbed rebars in normal strength concrete. Construction and Building Materials, 2009. 23(2):p. 865-871.
13. Bank, L.C., M. Puterman, and A. Katz, The effect of material degradation on bond properties of fiber reinforced plastic reinforcing bars in concrete. ACI Materials Journal, 1998. 95(3): p. 232-243.
14. Robert, M. and B. Benmokrane, Effect of aging on bond of GFRP bars embedded in concrete. Cement and Concrete Composites, 2010. 32(6): p. 461-467.
15. Abbasi, A. and P.J. Hogg, Temperature and environmental effects on glass fibre rebar: modulus, strength and interfacial bond strength with concrete. Composites Part B: Engineering, 2005. 36(5): p. 394-404
16. Bank, L., M. Puterman, and A. Katz, The effect of material degradation on bond properties of FRP reinforcing bars in concrete. ACI Materials Journal, 1998. 95: p. 232-243.

17. ACI Committee 549. (1997). State-of-the-Art Report on Ferrocement. ACI 549R-97, 1–26.
18. Hala Mohamed Refat Abd ElMohimen (2005) "Structural Behaviour of Ribbed Ferrocement Plate", B.SC. Thesis submitted to Menoufia University, Egypt.
19. Arshdeep Singh Channi (July 2009) "Effect of Percentage of Reinforcement on Beams Retrofitted with Ferrocement Jacketing", Thapar University Patiala-147004.
20. E.H. Fahmy, Y.B.I. Shaheen, A.M. Abdelnaby, M.N.A. Zeid, Applying the ferrocement concept in construction of concrete beams incorporating reinforced mortar permanent forms, *Int. J. Concr. Struct. Mater.* 8 (1) (2014) 83–97.
21. Y.B.I. Shaheen, E.A. Eltehawy, Structural behaviour of ferrocement channels slabs for low cost housing, *Challenge J. Concr. Res. Lett.* 8 (2) (2017) 48–64.
22. Bhattarai, B., Bhattarai, N. (2017). "Experimental study on flexural behavior of reinforced solid and hollow concrete beams". *International Journal of Engineering Research and Advanced Technology*, 3(11), 1-8.
23. P. Desayi, S.A. El-Kholy, Lightweight fibre-reinforced ferrocement in tension, *Cem. Concr. Compos.* 13 (1991) 37–48.
24. Salih, Y.A., Sabeeh, N.N., Yass, M.F., Ahmed, A.S., Abdulla, A.I, Behavior of ferrocement slabs strengthening with jute fibers under impact load ,(2020) *International Review of Civil Engineering*, 11 (2), pp. 66-72.
25. Erfan, A.M., Abd Elnaby, R.M., Elhawary, A. and El-Sayed, T.A., 2021. Improving the compressive behavior of RC walls reinforced with ferrocement composites under centric and eccentric loading. *Case Studies in Construction Materials*, 14, p.e00541.
26. El-Sayed, T.A. and Erfan, A.M., 2018. Improving shear strength of beams using ferrocement composite. *Construction and Building Materials*, 172, pp.608-617.
27. Erfan, A.M., Hassan, H.E., Hatab, K.M. and El-Sayed, T.A., 2020. The flexural behavior of nano concrete and high strength concrete using GFRP. *Construction and Building Materials*, 247, p.118664.